Available online at www.sciencedirect.com
ScienceDirect
Journal of Molecular Catalysis A: Chemical 260 (2006) 82–94
JOURNAL OF MOLECULAR CATALYSIS A: CHEMICAL
www.elsevier.com/locate/molcata

Development of chromium-free iron-based catalysts for high-temperature water-gas shift reaction

Sittichai Natesakhawat, Xueqin Wang, Lingzhi Zhang, Umit S. Ozkan *

The Ohio State University, Department of Chemical and Biomolecular Engineering, 140 W. 19th Avenue, Columbus, OH 43210, USA

Received 22 May 2006; received in revised form 3 July 2006; accepted 5 July 2006
Available online 17 August 2006

Abstract

Chromium-free iron-based catalysts were prepared and studied in regard to their performance in the high-temperature water-gas shift reaction (HTS). The effects of various catalyst preparation variables (i.e., Fe/promoter ratio, pH of precipitation medium, calcination and reduction temperatures) and preparation methods were investigated. Aluminum is a potential chromium replacement in HTS catalysts. Further improvement in WGS activity of Fe–Al catalysts can be achieved by the addition of small amounts of copper or cobalt. Catalysts were characterized using BET surface area measurements, temperature-programmed reduction (TPR), X-ray diffraction (XRD), X-ray photoelectron spectroscopy (XPS), and diffuse reflectance infrared Fourier transform spectroscopy (DRIFTS). As a textural promoter, aluminum and chromium prevent the sintering of iron oxides and stabilize magnetite phase by retarding its further reduction to FeO and metallic Fe. The promotional effect of Cu is found to be strongly dependent on the preparation method.

Keywords: Water-gas shift reaction; Iron-based catalysts; HTS catalysts; Chromium-free; Hematite; Magnetite; Sintering; Redox mechanism

1. Introduction

The water-gas shift (WGS) reaction is an important step in the production of H_2, where CO, which is produced from hydrocarbon steam reforming or coal gasification, is reacted with water to give H_2 and CO_2. The water-gas shift reaction is exothermic and thermodynamically limited at high temperatures:

$$CO\,(g) + H_2O(g) \Leftrightarrow CO_2\,(g) + H_2\,(g),$$

$$\Delta H(298\,K) = -41.2\,kJ/mol.$$

There has been renewed interest in the WGS reaction in recent years because of its necessity in conjunction with fuel cell power generation. The high-temperature shift (HTS) reaction is industrially performed at 320–450 °C using Fe–Cr oxide catalysts, while the low-temperature shift (LTS) reaction is conducted at 200–250 °C. The LTS catalysts commonly used are $Cu/ZnO/Al_2O_3$ or precious metal-based catalysts. The WGS reactor currently represents the largest volume of any catalyst in a fuel processor due to the slow kinetics at temperatures where the equilibrium is favorable [1].

Development of Fe–Cr catalysts with improved activity and stability has been pursued in the last two decades [2–16]. The existing WGS catalyst formulations still have many disadvantages such as their sensitivity to air and their low activity, which dictates higher temperature of operation, or large reactor volumes. Andreev et al. [3] studied the effect of the addition of CuO, CoO, and ZnO (5 wt.%) on the activity of Fe–Cr catalysts. The Cu-promoted sample was found to be the most active at 380 °C. Kappen et al. [13] investigated the state of the Cu promoter (0.17–1.5 wt.%) in Fe–Cr catalysts. It was found that Cu was in the metallic phase under the WGS reaction conditions. However, it reoxidized easily when exposed to the atmosphere. Rhodes et al. [14] examined the promotion of Fe–Cr catalysts with 2 wt.% B, Cu, Ba, Pb, Hg, and Ag. A beneficial effect of adding Hg, Ag, or Ba was observed between 350 and 440 °C. This could be due to their different ionic sizes compared to that of Fe^{2+}, influencing the electronic structure of the active Fe^{3+} center. Despite its high WGS activity, it is unlikely that the toxic Hg-promoted catalyst will be considered as a commercial HTS catalyst. Although Fe–Cr catalysts have been widely used in the HTS reaction, the

* Corresponding author. Tel.: +1 614 292 6623; fax: +1 614 292 3769.
E-mail address: ozkan.1@osu.edu (U.S. Ozkan).

1381-1169/$ – see front matter © 2006 Elsevier B.V. All rights reserved.
doi:10.1016/j.molcata.2006.07.013

role of the Cr_2O_3 addition on the stabilization of the catalyst structure is still unclear. Edwards et al. [15] proposed a model for the high stabilizing effect of chromium whereby a shell of chromium-enriched material is formed on each catalyst grain, but the mechanism by which promotion occurs is still uncertain.

It is known that the activation process can play an important role on the activity and stability of catalysts. Rethwisch et al. [17] investigated the effect of catalyst treatment on catalytic activity over 16.8 wt.% Fe_3O_4 supported on graphite. It was found that the treatment of the catalyst in CO/CO_2 at 390 °C prior to the reaction increased the WGS activity. In contrast, the catalyst treatment in H_2/H_2O caused the growth of magnetite particles, leading to a decrease in catalytic activity. Gonzalez et al. [4] studied the influence of thermal treatments and reduction processes on the WGS activity of Fe–Cr catalysts. The active phase, Fe_3O_4, can be obtained from partial reduction of Fe_2O_3. However, over-reduction to form metallic Fe should be avoided since it results in a loss of catalytic activity. The authors concluded that reduction under either H_2/N_2 or $CO/N_2/H_2/H_2O$ at temperatures below 500 °C should be performed to obtain higher activity without over-reduction of Fe_2O_3.

Even though chromium oxide has been used as a stabilizer in industrial HTS catalysts, its replacement with more benign components is highly desirable due to environmental concerns related to chromium. Araujo and Rangel [18] investigated the catalytic performance of Al-doped Fe-based catalyst with small amounts of copper (Cu ≈ 3 wt.%), prepared by coprecipitation–impregnation method, in the HTS reaction. The aluminum and copper-doped iron catalyst was studied at 370 °C and showed similar catalytic activity compared to the commercial Fe–Cr–Cu catalyst. Costa et al. [19] subsequently examined the use of thorium instead of chromium in iron- and copper-based catalysts for the HTS reaction. It was found that the thorium and copper-doped catalyst was more active than the commercial Fe–Cr–Cu catalyst at $H_2O/CO = 0.6$ and 370 °C. Its high activity was attributed to an increase in surface area by thorium.

In this study, we investigate the potential textural promoters for Cr replacement and structural promoters for enhancing the water gas shift activity of Fe-based catalysts. The catalyst preparation method is found to strongly affect the catalytic performance. Catalyst characterization was performed using BET surface area measurements, temperature-programmed reduction (TPR), X-ray diffraction (XRD), X-ray photoelectron spectroscopy (XPS), and diffuse reflectance infrared Fourier transform spectroscopy (DRIFTS). The catalytic activity was tested in a fixed bed flow reactor. The reaction mechanism of the HTS reaction over Fe-based catalysts is also examined.

2. Experimental

2.1. Catalyst preparation

All metal precursors (Aldrich) used were in nitrate form. Ammonium hydroxide (29.63 vol.%, Fisher Scientific) was used as the precipitating agent. Aluminum, manganese, and gallium were added into iron-based catalysts using a coprecipitation method. Initially, 0.5 M aqueous solutions of metal nitrates were prepared and mixed in a beaker in appropriate ratios to yield the desired Fe/promoter molar ratio. NH_4OH was subsequently added drop-wise to the mixed solution until the desired pH was reached. The resulting dark brown solution was stirred vigorously for an additional 30 min. The precipitate was washed with demineralized distilled water and filtered several times to remove ammonium ions. The remaining solid was then dried overnight in an oven at 110 °C. Catalysts promoted with first-row transition metals (Cu, Co, Zn) were synthesized by coprecipitation–impregnation (two-step) and one-pot coprecipitation (one-step) methods. In terms of two-step preparation, the washed precipitate obtained by coprecipitation was further impregnated with a calculated amount of 0.5 M aqueous solution of a first row transition metal and stirred for 30 min before drying. One-step catalysts were prepared by coprecipitating all components in one pot. Sodium carbonate was used as the precipitating agent instead of ammonium hydroxide to avoid the formation of copper ammonium complex at high pH value. The precipitate was centrifuged and washed with demineralized distilled water followed by dried overnight in an oven at 110 °C. All dried samples were ground to a fine powder and were calcined under air at 350–500 °C (ramp rate = 2.5 °C/min) for 4 h.

2.2. Catalyst characterization

BET surface areas of freshly calcined catalysts were measured by N_2 adsorption–desorption at 77 K using a Micromeritics ASAP 2010 instrument. Before measurements, samples were degassed under vacuum at 130 °C overnight. For *in situ* surface area measurements following reduction, AutoChem-2920 was used. In these experiments, surface area was measured before reduction, reduction step was performed, and the surface area was measured again, all in the same instrument. Temperature-programmed reduction (TPR) of catalysts was conducted using a laboratory-made gas flow system described in detail elsewhere [20]. First, 100 mg of catalyst was placed in a 1/4 in. o.d. quartz U-tube reactor. The catalyst was then re-calcined under 10% O_2/He at 450 °C for 1 h followed by cooling to room temperature under Ar. The reduction was performed with 10% H_2/Ar (40 cm^3 (STP)/min). The temperature of the catalyst was raised using a ramp rate of 10 °C/min to 950 °C and held for 30 min. The effluent from the reactor was passed through a silica gel water trap to remove moisture formed during reduction. H_2 consumption was measured using a thermal conductivity detector (TCD) connected to a data-acquisition computer.

X-ray powder diffraction (XRD) patterns of calcined catalysts were obtained with a Scintag XDS diffractometer using Cu Kα radiation (λ = 1.542 Å) operated at 45 kV and 20 mA. *In situ* X-ray powder diffraction (XRD) patterns were acquired by a Bruker D8 Advance X-Ray diffractometer equipped with atmosphere and temperature control (cryogenic to 1200 °C) capabilities and operated at 40 kV and 50 mA. The powder diffraction patterns were recorded in the 2θ range from 20° to 90°. Reduction was performed *in situ* under 5% H_2/N_2 gas flow using a linear temperature-program between isothermal steps. The cat-

alysts were kept at isothermal steps for 0.5 h and the ramp rate in between the isothermal steps was 10 °C/min.

X-ray photoelectron spectroscopy analysis (XPS) was performed using an AXIS Ultra XPS spectrometer, operated at 13 kV and 10 mA with Al Kα radiation (1486.6 eV). Reduced samples were treated at desired conditions for 2 h and then transferred to the XPS chamber using an inert-atmosphere transfer chamber without exposing them to the atmosphere. Charge neutralization was used to reduce effect of charge built on samples. All binding energies were referenced to C 1s binding energy of 284.5 eV.

Diffuse reflectance infrared Fourier transform spectroscopy (DRIFTS) experiments were performed using a Bruker IFS66 instrument equipped with DTGS and MCT detectors and a KBr beam splitter. Catalysts were placed in a sample cup inside a Spectratech diffuse reflectance cell equipped with KBr windows and a thermocouple that allowed direct measurements of the surface temperature. Prior to the collection of spectra, the catalyst was reduced *in situ* under CO/H_2O at 350 °C for 2 h followed by flushing under He for 30 min. The background spectra were taken under He at different temperature intervals.

2.3. Reaction studies

Reaction experiments were performed using a fixed-bed flow system with a stainless steel reactor (1/4 in. o.d.). The reaction conditions were as follows: 250–450 °C, $CO/H_2O/N_2 = 1/1/8$ (the ratio of CO/H_2O is the same as that in coal-derived Syngas), feed flow rate = 100 cm^3 (STP)/min. Unless otherwise noted, catalysts were reduced *in situ* under 20% H_2/N_2 (50 cm^3 (STP)/min) at 350 °C for 2 h prior to the reaction. The feed and effluent streams were analyzed on-line using an automated Shimadzu GC-14A equipped with FID and TCD detectors and a methanizer. Separation of species was performed under Ar using 2 columns: Porapak Q (12 ft × 1/8 in. SS, 80/100 mesh) and molecular sieve 13X (5 ft × 1/8 in. SS, 60/80 mesh).

3. Results and discussion

3.1. Studies on textural promoters

3.1.1. Replacement of chromium

It is believed that the function of chromium in commercial HTS formulations is to keep magnetite from sintering, thus enhancing the activity and stability of iron catalysts [21,22]. However, the use of chromium poses additional complications due to harmful effects of Cr^{6+} on human health such as cancer risk and lung damage [23]. Therefore, development of chromium-free catalytic systems is necessary. There appears to be a general consensus that chromium is incorporated into the hematite lattice to form a solid solution instead of segregating into a separate phase. It is, therefore, conceivable that any metal that has an ionic radius similar to Fe^{3+} (0.69 Å) could easily be incorporated into the hematite lattice. Based on this concept, aluminum, manganese, and gallium were chosen to replace chromium. The ionic radii of metals investigated in this study are as follows: Al^{3+} (0.675 Å), Mn^{3+} (0.72 Å), Cr^{3+} (0.755 Å), Ga^{3+} (0.76 Å) [24]. Although the main function of Cr is generally thought to be that of a textural promoter, keeping magnetite from sintering, it is possible that part of Cr species may also act as active sites. Al_2O_3 is widely used in F–T catalyst [25] as spacers to protect iron catalyst from sintering because of its high thermal and chemical stability. Its use as a textural promoter for WGS catalyst was also reported [18]. The preliminary tests (Table 1) showed that Fe–Al demonstrated higher activity than Fe-only, Fe–Ga and Fe–Mn, although Cr-containing catalyst still had higher activity. Also shown in Table 1 are the surface area measurements of the hematite phase. For Cr and Al containing catalysts, higher surface areas correspond to higher activity. However, such a trend is not apparent in Fe–Ga and Fe–Mn containing catalysts. The post-reduction surface areas of the three most active catalysts are also included in Table 1 for comparison. There is a loss of surface area in all three samples; however, Fe-only catalyst had the largest percent decrease in surface area (∼34%). To optimize the promotional effect of Al_2O_3, effects of various synthesis variables (i.e., Fe/Al molar ratio, pH of precipitation medium) on the activity and stability of the catalysts were examined.

3.1.1.1. Effect of Fe/Al molar ratio. A first series of Fe–Al catalysts was prepared at differing Fe/Al molar ratios from 5 to 20. The pH value of the precipitation medium and calcination temperature were kept constant at 9 and 450 °C, respectively. Table 2 shows that the WGS activity of Fe–Al catalysts increases with decreasing Fe/Al molar ratio (or at higher Al contents) and reaches a maximum at Fe/Al = 10. Further addition of Al (Fe/Al = 5) causes a significant drop in WGS activity possibly

Table 1
BET surface area measurements and % CO conversion over Fe-based catalysts with different textural promoters

Catalyst[a]	Surface area (m^2/g)		CO conversion (%)		
	Pre-reduction	Post-reduction	350 °C	400 °C	450 °C
Fe-only	19	12	8	20	27
Fe–Cr	54	43	19	43	56
Fe–Al	61	54	11	27	43
Fe–Ga	31	NA	NA	12	NA
Fe–Mn	64	NA	NA	16	NA
Equilibrium conversion			73	78	82

[a] Synthesis variables: Fe/Al (Cr, Ga, Mn = 10), pH 9, T_{cal} = 450 °C. Reduced at 350 °C with 20% H_2/N_2 for 2 h.

Table 2
Effect of synthesis parameters on the high-temperature water-gas shift reaction activity of Fe–Al catalysts[a]

Fe/Al	pH	T_{cal} (°C)	CO conversion (%)
5	9	450	14
10	9	450	25
15	9	450	18
20	9	450	16
10	8	450	13
10	9	450	25
10	10	450	20
10	11	450	15
10	9	350	16
10	9	400	19
10	9	450	25
10	9	500	22

[a]Reaction conditions: 400 °C, $CO/H_2O/N_2 = 1/1/8$, feed flow rate = 100 cm^3 (STP)/min, equal weight reactions (0.1 g), *in situ* reduction at 350 °C under 20% H_2/N_2 for 2 h.

due to segregation of aluminum into a separate phase or a dilution effect that Al may have on Fe sites.

3.1.1.2. Effect of pH of the precipitation medium. A second series of Fe–Al catalysts was subsequently prepared by varying the pH values of the precipitation medium. The Fe/Al molar ratio and calcination temperature were kept constant at 10 and 450 °C, respectively (Table 2). The pH value is one of the major factors to control the precipitation rate of different species in the mixture of catalyst precursors. Lower pH value of the precipitation medium could favor the precipitation of iron species whereas the precipitation rate of aluminum species becomes faster at higher pH values. Reaction results indicate that the optimum pH value of the precipitation medium is 9 to get the highest activity of Fe–Al catalyst. This finding is different from an earlier study which reported using a pH 11 for catalyst preparation [18]. Our experiments show that precipitated Al species starts to dissolve in water when pH is over 9.

3.1.1.3. Effect of calcination temperature. A third series of Fe–Al catalysts was synthesized at Fe/Al = 10 and pH 9. CO conversion levels of Fe–Al catalysts prepared at various calcination temperatures ranging from 350 to 500 °C are also listed in Table 2. The catalytic activity of Fe–Al catalysts is seen to go through a maximum at 450 °C. Higher calcination temperature results in a decrease in WGS activity possibly due to loss of surface area caused by sintering.

3.1.2. Role of Al as a textural promoter

3.1.2.1. Temperature-programmed reduction. To examine the change in catalyst reducibility with promotion, TPR was performed with 10% H_2/Ar over Fe-only and Fe-promoted by Al- and Cr-promoted Fe catalysts calcined at 450 °C. As depicted in Fig. 1, there are two main reduction features observed for the Fe-only catalyst. A low-temperature (LT = 420 °C) feature is assigned to the reduction of hematite (Fe_2O_3) to magnetite (Fe_3O_4). A broad high-temperature (HT) feature is attributed to

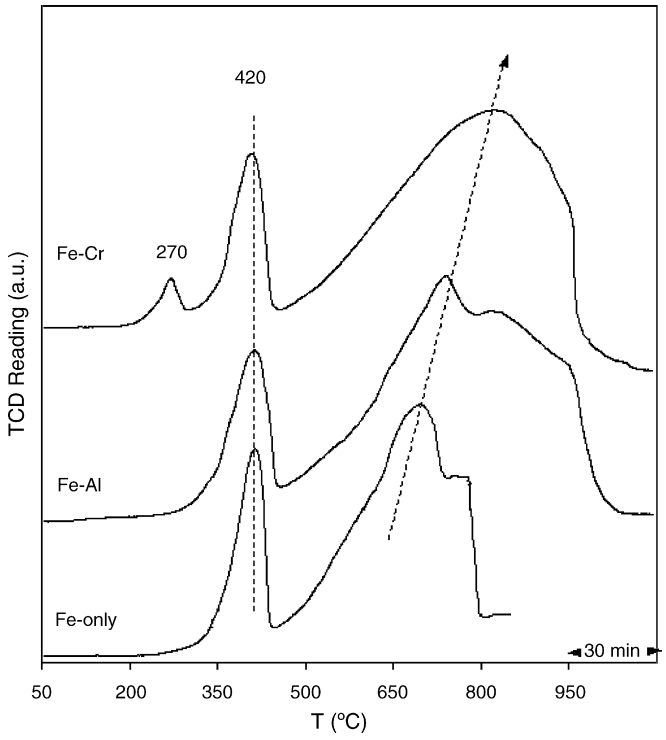

Fig. 1. TPR profiles of Fe-based catalysts promoted with textural promoters.

the reduction of magnetite (Fe_3O_4) to FeO/Fe. The addition of Al and Cr into iron catalysts does not affect the LT significantly, while it leads to a shift of the HT peak maximum to higher temperatures. This suggests that the addition of Al and Cr stabilizes magnetite and prevents its further reduction to undesirable FeO or metallic Fe. An additional reduction peak, assigned to the reduction of Cr^{6+} to Cr^{3+} [4], is seen at 270 °C for Fe–Cr catalyst. There is no reduction feature due to reduction of Al species in the Fe–Al catalyst.

3.1.2.2. XRD studies on calcined catalysts. The XRD patterns of catalysts calcined at 450 °C are displayed in Fig. 2. Hematite

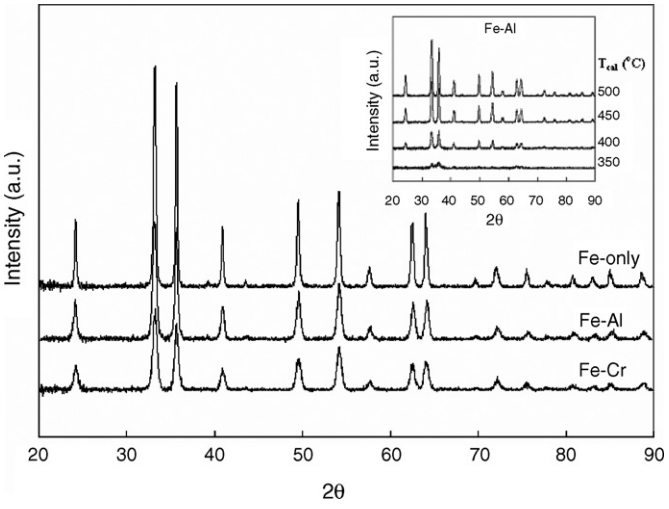

Fig. 2. XRD patterns of Fe-based catalysts promoted with textural promoters (calcined at 450 °C). The effect of calcination temperature on crystallinity of Fe–Al catalysts is shown as an inset.

(Fe_2O_3) is the only crystalline phase detected. No separate Al- and Cr-containing crystalline phases are observed on the calcined samples, suggesting that Al and Cr could exist in a solid solution within the hematite matrix or as amorphous phases. XRD diffraction lines of all promoted catalysts are much broader than Fe-only catalyst, suggesting that hematite crystallites in these catalysts are significantly smaller. The crystallite sizes of hematite were further compared by calculating them from line broadening of Fe_2O_3(1 0 4) diffraction line using the Scherrer equation [26]. As shown in Table 3, the addition of Al and Cr in Fe catalysts helps improve the sintering resistance of hematite as confirmed by much smaller crystallite sizes of hematite at all calcination temperatures. In addition, the effect of calcination temperature on the crystallinity of Fe–Al catalysts is shown as an inset in Fig. 2. The catalyst calcined at 350 °C is relatively amorphous. As the calcination temperature is increased, Fe–Al catalysts become more crystalline.

3.1.2.3. In situ XRD studies during reduction. Phase transformations that took place during reduction in Fe-based catalysts were further investigated by an *in situ* XRD technique. The corresponding *d* spacings and (*h k l*) values for the diffraction lines of iron-containing species using the International Centre for Diffraction Data (ICDD) PDF database are given in Table 4. As seen in Fig. 3, no phase transformation occurs in Fe–Al catalyst below 250 °C; the only crystalline phase observed is hematite. At 300 °C, hematite begins to reduce to magnetite (Fe_3O_4), which is further reduced to FeO above 600 °C. When the Fe, Fe–Al, and Fe–Cr catalysts are compared, there is no difference in the temperature at which magnetite phase first appeared during reduction. This temperature is 300 °C for all three catalysts. For further reduction of the magnetite phase however, there are significant differences. In Fe-only catalyst, FeO is detected at a much lower reduction temperature (500 °C) compared to Fe–Al (600 °C) and Fe–Cr (700 °C) catalysts. There was no crystalline metallic Fe phase in any of the catalysts. The presence of Al and Cr in Fe catalysts stabilizes the magnetite phase and prevents its further reduction to FeO. This is in good agreement with the TPR results. The crystallite sizes of various Fe-based catalysts reduced at different temperatures (300–450 °C) were calculated from line broadening of Fe_3O_4 (3 1 1) diffraction line and are listed in Table 5. It can be seen that magnetite crystallite sizes increase with increasing reduction temperature, but the presence of Al and Cr significantly inhibits the growth of magnetite crystallites.

Table 3
Effect of calcination temperature on hematite crystallite size of Fe-based catalysts

Catalyst	*d* (nm) at different calcination temperature			
	350 °C	400 °C	450 °C	500 °C
Fe	37	39	51	60
Fe–Al	n.d.[a]	29	33	37
Fe–Cr	n.d.[a]	25	27	40

[a] Not determined since Fe_2O_3(1 0 4) diffraction line was not well resolved.

Table 4
Major peaks in the XRD patterns of identified phases during *in situ* reduction of Fe-based catalysts

Phase	*d* (Å)	2*θ*	(*h k l*)
Fe_2O_3	3.684	24.14	(0 1 2)
	2.700	33.15	(1 0 4)
	2.519	35.61	(1 1 0)
	2.207	40.85	(1 1 3)
	1.841	49.48	(0 2 4)
	1.694	54.09	(1 1 6)
	1.599	57.59	(0 1 8)
	1.486	62.45	(2 1 4)
	1.454	63.99	(3 0 0)
	1.306	72.26	(1 1 9)
Fe_3O_4	2.967	30.09	(2 2 0)
	2.532	35.42	(3 1 1)
	2.099	43.05	(4 0 0)
	1.715	53.39	(4 2 2)
	1.616	56.94	(5 1 1)
	1.485	62.51	(4 4 0)
FeO	2.490	36.04	(1 1 1)
	2.153	41.92	(2 0 0)
	1.523	60.76	(2 2 0)
	1.299	72.73	(3 1 1)
	1.243	76.58	(2 2 2)
Fe	2.027	44.67	(1 1 0)
	1.433	65.02	(2 0 0)

3.1.2.4. XPS studies on calcined and reduced catalysts. In order to investigate the nature of active sites and oxidation states of species upon reduction, XPS was performed over calcined and reduced catalysts. The Fe 2p spectra for all calcined samples were identical, therefore only one representative spectrum

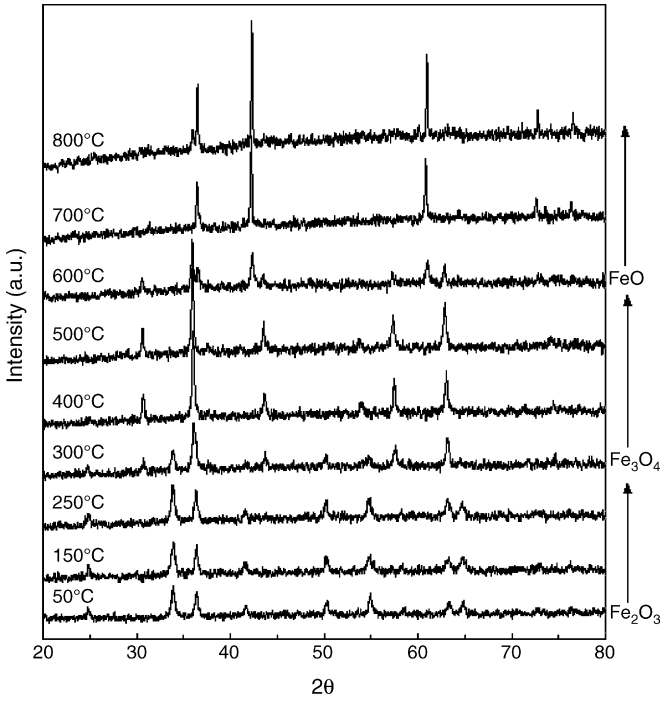

Fig. 3. *In situ* XRD patterns during reduction of Fe–Al catalyst.

Table 5
Effect of reduction temperature on magnetite crystallite diameter of Fe-based catalysts

Catalyst	*d* (nm) at different reduction temperatures			
	300 °C	350 °C	400 °C	450 °C
Fe	54	69	70	77
Fe–Al	36	51	52	58
Fe–Cr	35	57	59	60

(Fe-only catalyst calcined at 450 °C, O-450-Fe) was included in Fig. 4. Hematite (710.9 eV) is the only iron species observed on the surface of calcined catalysts at 450 °C. After reduction at 350 °C, all peaks shift to lower binding energies. It should be noted that reduction with H_2 could lead to over reduction. In fact, it is not necessarily how the functioning catalysts are pretreated. However, in order to see the differences that result from the promotional effect of Al and Cr, a "harsher" reduction procedure was used. Effect of the reduction process using different reduction media will be discussed in the following sections.

It appears that magnetite (710.4 eV) is the major species detected over all reduced catalysts, although FeO may also be present. The most striking feature, however, is seen at 706.6 eV, over the Fe-only catalyst reduced at 350 °C, signaling the presence of metallic iron. The peak intensity of surface metallic iron is markedly suppressed on both Fe–Cr and Fe–Al catalysts. Consistent with TPR and *in situ* XRD results, the addition of Al and Cr in Fe catalysts helps stabilize the magnetite phase and keeps it from further reduction.

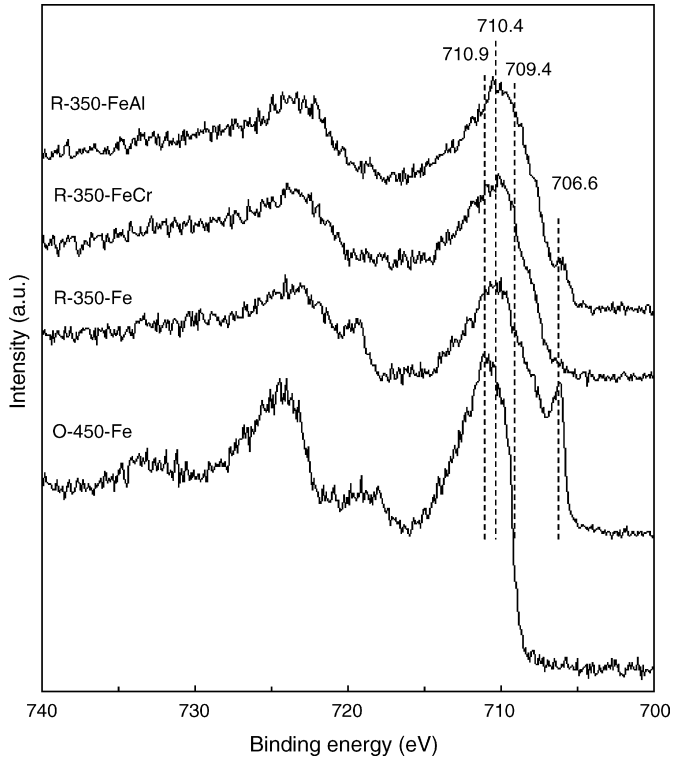

Fig. 4. X-ray photoelectron spectra (Fe 2p region) of (reduced at 350 °C, 20% H_2/N_2, 2 h) Fe-based catalysts promoted with textural promoters.

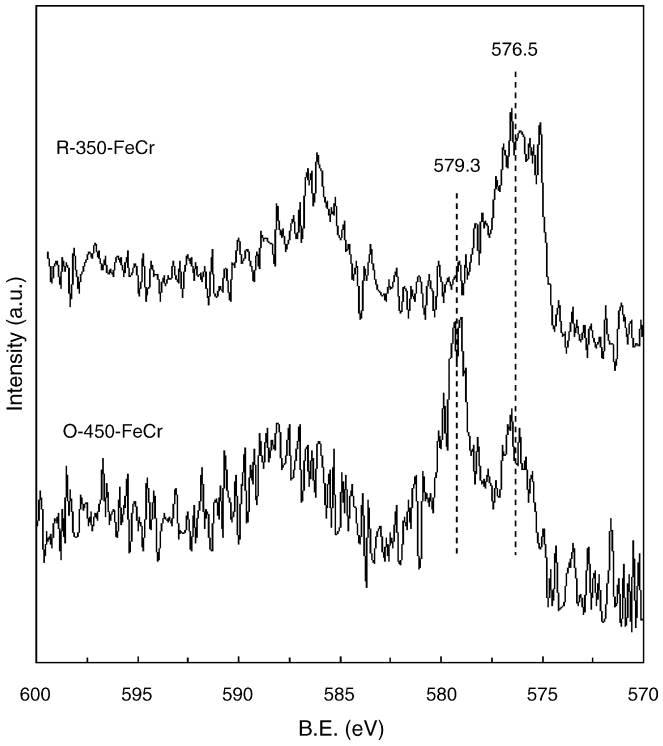

Fig. 5. X-ray photoelectron spectra (Cr 2p region) of calcined and reduced Fe–Cr catalysts.

Fig. 5 shows the Cr 2p region of the X-ray photoelectron spectrum. Cr species is found to have two oxidation states in the calcined sample: Cr^{6+} (579.3 eV) and Cr^{3+} (576.5 eV). After reduction at 350 °C, Cr^{6+} is reduced to Cr^{3+}, which was also observed in the TPR profile of Fe–Cr catalyst. The existence of two oxidation states may facilitate a reduction–oxidation function for Cr species and may play a role in promoting the WGS reaction, which proceeds through a redox cycle. This property could partially explain why Cr-promoted iron catalyst possesses significantly higher activity. There was no change in the Al 2p spectra after reduction (not shown).

3.2. Studies on structural promoters

The role of a structural promoter is generally to increase the catalytic activity by creating/providing new active sites or affecting the structural (e.g., electronic) properties. In this study, Fe–Al catalysts were promoted with first-row transition metals (copper, cobalt, zinc) using an impregnation method. Prior to promotion, the catalysts were prepared by coprecipitation of Fe and Al species, at a constant Fe/Al ratio of 10. Because of the two steps involved in the preparation, this method is referred to as "two-step preparation". In the first comparison of the promoted catalysts, the Fe/promoter ratio constant was kept constant at 20. As shown in Table 6, although addition of Zn does not provide any higher activity compared to Fe–Al catalyst, promotion with Co and Cu leads to significantly higher CO conversions, with Fe–Al–Cu catalyst giving the highest activity. The promotion of Fe catalysts is seen to increase the surface area (Table 6), although it appears that the change in activity with the promot-

Table 6
BET surface area measurements and % CO conversion over Fe–Al catalysts: effect of structural promoters

Catalyst[a]	Surface area (m^2/g)	CO conversion (%)[b]
Fe–Al	61	25
Fe–Al–Zn (two-step)	78	19
Fe–Al–Co (two-step)	84	34
Fe–Al–Cu (two-step)	88	46

[a] Synthesis variables: Fe/Al (Cr, Ga, Mn = 10), Fe/Cu (Co, Zn) = 20, pH 9, T_{cal} = 450 °C.
[b] Reaction conditions: 400 °C, $CO/H_2O/N_2$ = 1/1/8, feed flow rate = 100 cm^3 (STP)/min, equal weight reactions (0.1 g), *in situ* reduction at 350 °C under 20% H_2/N_2 for 2 h.

ers cannot be explained solely by the variation in surface area since Fe–Zn has a higher surface area than the Fe-only catalyst, but it has a lower activity. Copper was reported to be a good promoter for Fe–Cr [3,13,14] and Fe–Al [18] catalysts in WGS reaction by other researchers. As shown in Table 7, the WGS activity of Fe–Al–Cu catalysts increases with decreasing Fe/Cu molar ratio (or at higher Cu contents) until it reaches a maximum at Fe/Cu = 20. A further decrease in Fe/Cu molar ratio causes a drop in WGS activity.

3.2.1. Temperature-programmed reduction

To examine the change in catalyst reducibility with incorporation of first row metals and through different preparation methods, TPR was performed with 10% H_2/Ar over catalysts calcined at 450 °C (Fig. 6). Over Fe–Al–Co and Fe–Al–Zn catalysts, three main reduction peaks were observed in TPR profiles including a shoulder peak at low temperature, a sharp peak due to reduction of hematite to magnetite, and a broad peak resulting from reduction of magnetite to FeO or/and metallic Fe. Fe–Al–Cu (two-step) catalyst shows three main reduction features with a strong and well-resolved reduction peak from Cu species at around 220 °C. After incorporation of first row transition metal promoters onto Fe–Al catalysts with the two-step preparation, both reduction peaks of hematite to magnetite and magnetite to FeO/Fe shift to lower temperatures comparing with those from Fe–Al catalyst. It implies that promotion with first row transition metals enhance the reducibility of the hematite phase. It is possibly due to the promotion of hydrogen dissociation over Cu, Co or Zn metallic species (after reduction).

Table 7
Effect of Cu content on the activity of Fe–Al–Cu catalysts[a,b]

Catalyst	Fe/Cu	CO conversion (%)
Fe–Al	–	25
Fe–Al–Cu	10	40
Fe–Al–Cu	20	46
Fe–Al–Cu	30	42
Fe–Al–Cu	40	37

[a] Preparation conditions: Fe/Al = 10, pH 9, calcination temperature = 450 °C.
[b] Reaction conditions: 400 °C, $CO/H_2O/N_2$ = 1/1/8, feed flow rate = 100 cm^3 (STP)/min, equal weight reactions (0.1 g), *in situ* reduction at 350 °C under 20% H_2/N_2 for 2 h.

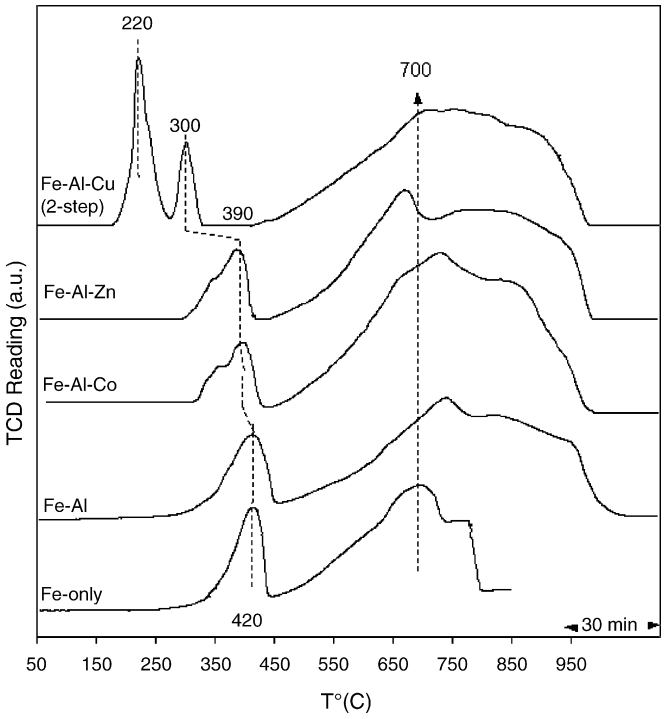

Fig. 6. TPR profiles of Fe–Al-based catalysts promoted with first row transition metal species.

3.3. Studies on Fe–Al–Cu catalysts

3.3.1. Effect of preparation method

Further studies were focused on Cu-promoted catalysts. The way Cu is incorporated into the catalyst was changed by introduction of a one-step preparation technique. In contrast to Fe–Al–Cu (two-step) catalysts that were prepared by impregnating Cu species onto Fe–Al sample synthesized using coprecipitation method, Fe–Al–Cu (one-step) catalysts were prepared with a "one-pot coprecipitation" method where starting chemicals were mixed all at once. Sodium carbonate was used as a precipitating agent instead of ammonia hydroxide because Cu species react with ammonium hydroxide to form a soluble complex at high pH values. Fig. 7 shows a comparison of CO conversion

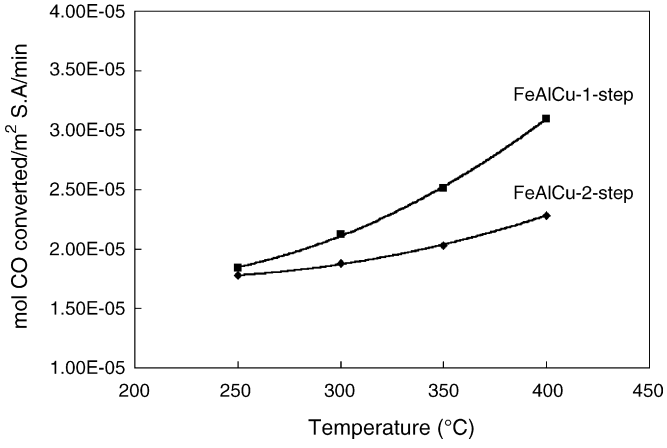

Fig. 7. Effect of preparation method on Fe–Al–Cu catalysts prepared using two-step and one-step methods.

rates for Fe–Al–Cu (two-step) and Fe–Al–Cu (one-step) catalysts at different reaction temperatures. Although the activities are similar at 250 °C, at higher temperatures, Fe–Al–Cu (one-step) catalyst shows a higher activity.

A significant difference in TPR profiles was observed between Fe–Al–Cu catalysts prepared by one-step and two-step methods (Fig. 8). Although it is not well-resolved, it appears that the low-temperature reduction feature has contributions from three different reduction sites. The reduction of hematite to magnetite appears to have shifted from 300 to 290 °C. The major peak from reduction of Cu species appears at 260 °C with a very weak shoulder around 220 °C. This shoulder peak is possibly due to the reduction of Cu species which are on the catalyst surface and which can be reduced very easily. The rest of the copper species appear to be more difficult to reduce as seen by a shift in reduction temperature from 220 to 260 °C, possibly due to stronger interaction with the hematite matrix. While the peak resulting from reduction of hematite to magnetite shifts to lower temperatures (from 300 to 290 °C), the peak from further reduction of magnetite changes very little compared to unpromoted Fe–Al catalyst. These results suggest that the preparation method makes a significant difference in the way Cu promoter is incorporated into the catalyst structure.

3.3.2. *In situ* XRD studies during reduction

Phase transformations that took place during the reduction of Fe–Al-Cu catalysts were investigated by an *in situ* XRD technique and the results are presented in Fig. 9. No phase transformation occurs in Fe–Al–Cu (one-step) catalyst below 200 °C; the only crystalline phase observed is hematite. Magnetite (Fe_3O_4) appears at 250 °C and it is stable up to 550 °C. At

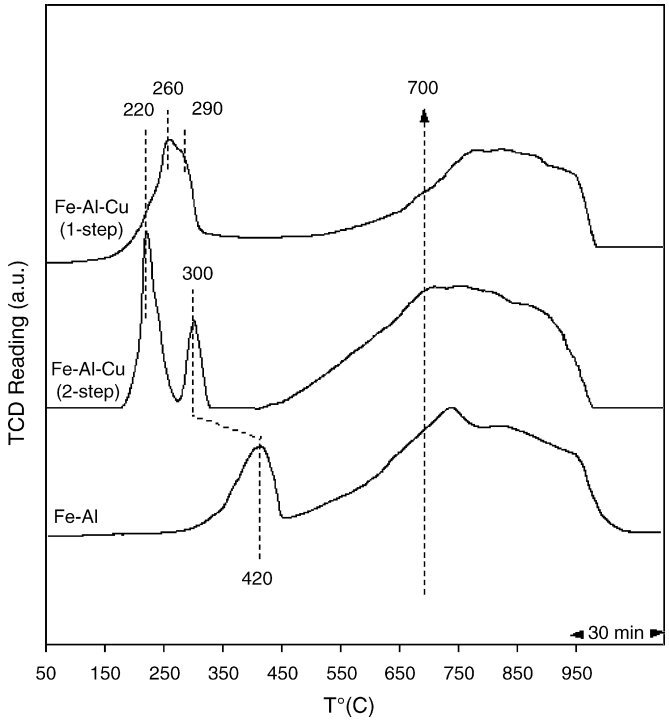

Fig. 8. Effect of preparation methods on the TPR profiles of Fe–Al–Cu catalysts.

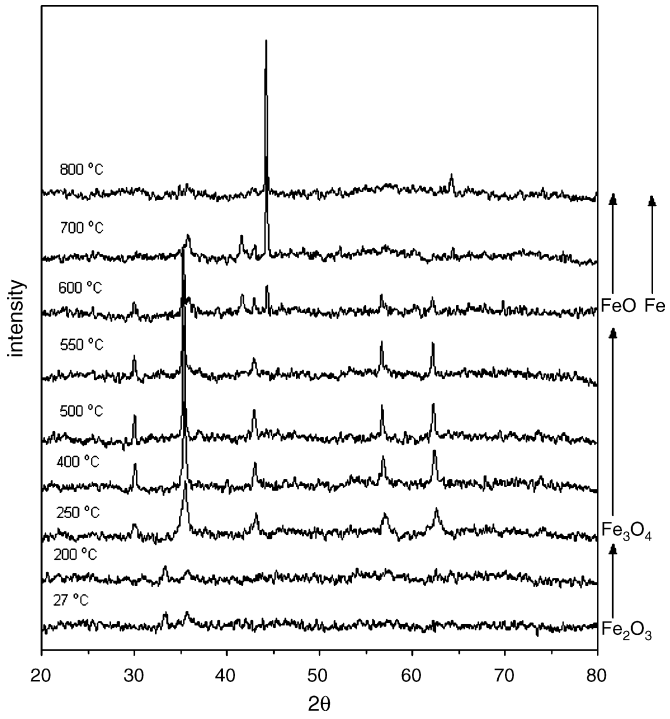

Fig. 9. *In situ* XRD patterns during reduction of Fe–Al–Cu (one-step) catalyst.

600 °C, FeO and metallic Fe appear simultaneously. The intensity of metallic Fe increases quickly with increasing reduction temperature, while intensity of FeO decreases gradually. When the temperatures at which phase transformations take place during reduction are compared, we see that the addition of Cu lowers the temperature for magnetite formation to 250 °C as opposed to the 300 °C for the Fe–Al catalyst. No FeO phase was observed over the Fe–Al–Cu (two-step) catalyst although metallic Fe phase appears at lower temperatures (450 °C) compared to Fe–Al–Cu (one-step) catalyst. This finding is consistent with the TPR results that the surface metallic Cu enhances the reduction of magnetite to FeO/Fe. FeO phase is not stable at low temperatures and decomposes into metallic iron [27,28]. With the surface Cu enhancement, it is found to reduce more easily to metallic Fe. Nevertheless, the characteristics imparted by Al incorporation (i.e., ease of reduction of the hematite phase and the stability of the magnetite phase up to 600 °C) are still intact in the Fe–Al–Cu (one-step) catalyst. The crystallite sizes of magnetite reduced at different temperatures (300–450 °C) are listed in Table 8 for Fe–Al–Cu catalysts. It can be seen that magnetite crystallite sizes of Fe–Al–Cu catalysts are smaller than the Fe–Al catalysts. Between the two preparation steps, the

Table 8
Effect of reduction temperature on magnetite crystallite diameter of Fe-based catalysts

Catalyst	*d* (nm) at different reduction temperatures			
	300 °C	350 °C	400 °C	450 °C
Fe–Al	36	51	52	58
Fe–Al–Cu (two-step)	26	36	41	41
Fe–Al–Cu (one-step)	18	20	28	32

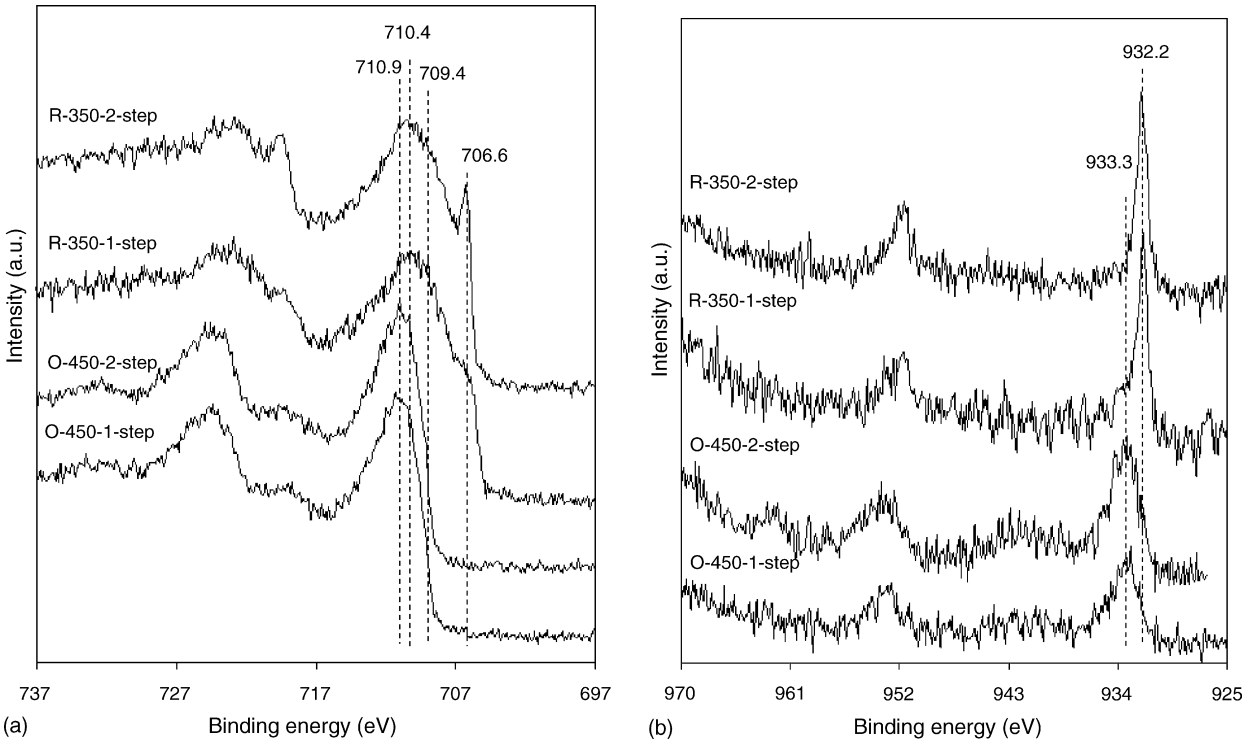

Fig. 10. X-ray photoelectron spectra of calcined and reduced Fe–Al–Cu catalysts prepared using two-step and one-step methods: (a) Fe 2p region; (b) Cu 2p region.

one-step preparation appears to give smaller crystallite sizes for magnetite.

3.3.3. XPS studies on Fe–Al–Cu catalysts

Fig. 10 shows the XPS spectra of Fe 2p and Cu 2p over calcined (450 °C) and reduced (350 °C) Fe–Al–Cu catalysts prepared by one-step and two-step preparation. In Fe 2p region, the spectra for calcined one-step and two-step catalysts are practically the same, showing a binding energy typical of the hematite phase (Fe $2p_{3/2}$ = 710.9 eV). After reduction at 350 °C for 2 h, the peak center shifts to lower binding energies (710.9–710.4 eV), which is characteristic of magnetite. Both catalysts reduced at 350 °C showed the presence of metallic Fe on the surface with a binding energy of 706.6 eV, however this feature was much more prominent in the two-step preparation. The sample prepared by the one-step technique only showed a shoulder at this binding energy, indicating that the surface composition of metallic Fe is much lower over this catalyst. Cu 2p spectra of calcined Fe–Al–Cu catalysts prepared by one-step and two-step are very similar (Fig. 10b), which is the characteristic of CuO species (Cu $2p_{3/2}$ = 933.3 eV), except that two-step sample shows a higher quantity of surface Cu species. After reduction at 350 °C, Cu species is converted to metallic copper (932.2 eV). However, a shoulder feature at higher binding energy clearly exists over the sample prepared by the one-step technique, which may imply that a small amount of Cu species is incorporated into iron oxide matrix and cannot be reduced to the metallic phase.

3.3.4. Effect of the reduction step

Fig. 11 shows the conversion of CO and H_2O versus time-on-stream for Fe–Al–Cu (one-step) catalysts undergone three different pretreatments, namely pre-reduction with 20%H_2/N_2 at 350 °C, pre-reduction with CO/H_2O at 350 °C, and no pre-reduction. The reaction temperature for all three runs were 400 °C. The catalyst pre-reduced with 20%H_2/N_2 shows the lowest steady-state conversions of CO and H_2O, while the catalyst pre-reduced with CO/H_2O at 350 °C exhibits the highest steady-state activity. The one which has undergone no pre-reduction gives a steady-state performance in between. Another interesting feature to note in this figure is the difference between the conversion of CO and H_2O during the first two hours of reaction. For the catalyst pre-reduced with hydrogen, the initial conversion of H_2O is much higher than that at steady-state. The extra consumption of H_2O at the beginning of reaction is caused by the oxidation of metallic Fe, as will be discussed in the next

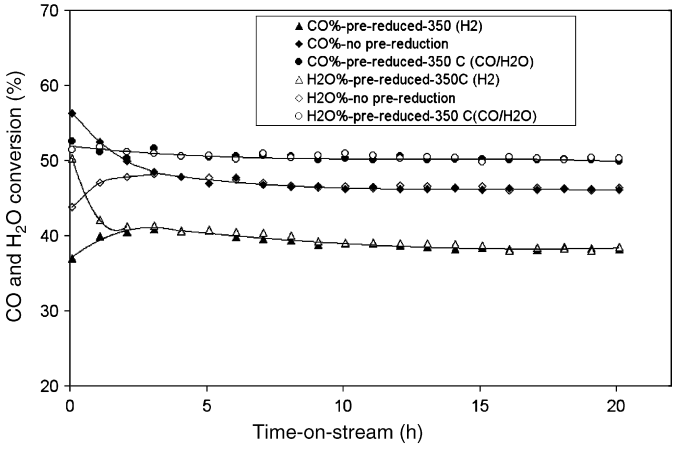

Fig. 11. Effect of reduction steps on catalytic performance of Fe–Al–Cu (one-step) catalyst: conversion of CO and H_2O vs. time-on-stream.

section. The initial CO conversion, on the other hand, is lower than that at steady-state. It is caused by the lower H_2O concentration available for the water gas shift reaction since part of H_2O is consumed through reaction with metallic Fe. Conversion of H_2O and CO reaches the same level after about one hour on stream. For the catalyst which is pre-reduced using CO/H_2O, the conversions of H_2O and CO are at the same level from the beginning of the reaction and remain steady during the time-on-stream over 20 h. The CO and H_2O conversion levels over the catalyst without any pre-reduction show opposite trends during the first two hours. Initially, CO conversion is significantly higher than H_2O conversion. This initial high conversion of CO results from its consumption through the reduction of the hematite phase. As more and more of the hematite phase gets reduced to the magnetite phase, the water gas shift reaction rate increases and the conversion levels for CO and H_2O become equal at steady-state. However, the steady-state activity is lower than that over the catalyst pre-reduced at 350 °C. Actually, the catalyst without pre-reduction goes through *in situ* reduction during the first few hours of the reaction, hence, it can be considered to be pre-reduced at 400 °C. Therefore, the catalyst pre-reduced at high temperature (400 °C) shows lower activity than that pre-reduced at low temperature (350 °C). This observation suggests that the catalyst could be over-reduced at high temperatures, resulting in a decrease in the magnetite active phase. The lowest activity of catalyst pre-reduced with H_2/N_2 reveals that it is crucial to add steam to hydrogen to prevent consecutive reduction of magnetite to FeO or Fe.

Fe 2p regions of the XPS spectra taken over Fe–Al–Cu (two-step) catalyst reduced with different agents and at different temperatures are shown in Fig. 12a. In addition to the magnetite phase (Fe $2p_{3/2}$ = 710.4 eV), those catalysts that were reduced without water in the reduction gas mixture exhibited metallic Fe (Fe $2p_{3/2}$ = 706.6 eV), regardless of whether the reducing agent was CO or H_2. The metallic Fe peak was much more pronounced over the sample reduced with CO/N_2 compared to the one reduced with H_2/N_2 mixture. This is to be expected since CO is a much stronger reducing agent than H_2. When reduction was performed with a gas mixture that contains water, the main feature is at 710.4 eV, which implies that the major iron species in the catalyst is magnetite. The existence of steam in the reduction mixture prevents further reduction of magnetite to FeO/Fe.

A similar comparison was made over the Fe–Al–Cu (one-step) catalysts using reducing agents with and without water. Fig. 12b shows the Fe 2p region of the X-ray photoelectron spectra taken following the reduction steps. The observations made for the two-step catalysts still hold in this case. Reduction using dry reducing agents lead to over reduction. One interesting point to note is that the one-step catalyst which is reduced with dry H_2, shows a very weak shoulder for the metallic Fe, whereas this feature was much more prominent in the two-step catalyst reduced under similar conditions. Comparing the spectra of catalysts reduced at 400 and 350 °C with CO/H_2O (Fig. 12b), it can be seen that the bands are much broader when the catalyst is reduced at 400 °C, possibly exhibiting some FeO/Fe on the

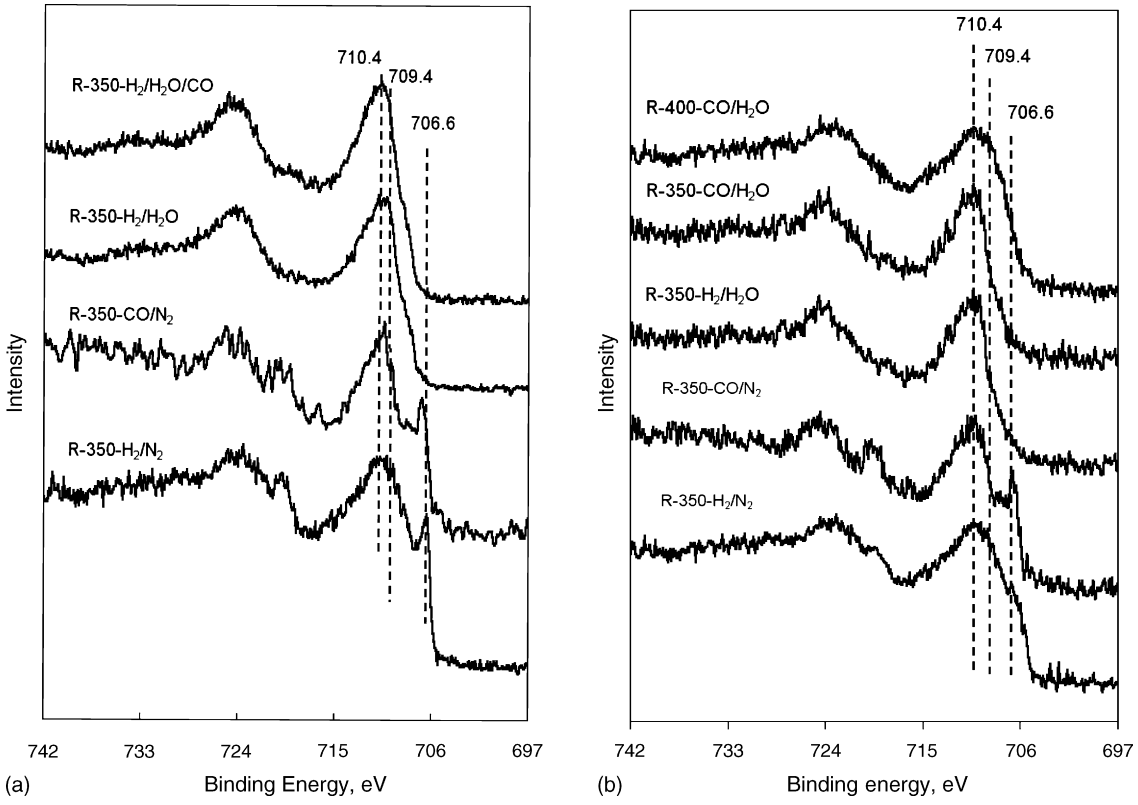

Fig. 12. X-ray photoelectron spectra of Fe–Al–Cu catalysts reduced with different reducing agents and at different temperatures: (a) two-step catalyst; (b) one-step catalyst.

surface, which is formed from over-reduction of the catalyst at high temperature. Reaction results combined with the XPS findings reiterate that the most active iron phase for the water gas shift reaction is magnetite.

3.4. DRIFTS studies on the redox cycle

Fig. 13 shows surface and gas phase species formed as a result of CO adsorption and water gas shift reaction over reduced Fe–Al–Cu (one-step) catalysts studied with the DRIFTS technique. At the beginning of the experiment, CO was flowed over the catalyst surface at room temperature. During CO flow at room temperature, two strong bands at 2173 and 2110 cm^{-1} are observed, which are assigned to gas-phase CO and weakly adsorbed CO, respectively [29–31]. Following He flushing at room temperature, the band at 2173 cm^{-1} disappears completely. The intensity of the band at 2110 cm^{-1} decreases rapidly with increasing temperature and disappears at 200 °C, indicating weak adsorption of CO on the catalyst surface. After the catalyst was heated to 400 °C under He flow, a stream of CO–H_2O was introduced to the system and subsequent spectra were collected under CO–H_2O flow at 400 °C. As soon as CO–H_2O mixture is introduced, a strong doublet at 2358 and 2327 cm^{-1} appears, signaling the formation of CO_2. The intensity of these bands decreases slightly in the first 30 min whereas the intensity of the CO bands (2173 and 2110 cm^{-1}) increases simultaneously. After about 30 min, the intensities of CO and CO_2 remain constant, indicating that steady-state is reached under these conditions. Following the water gas shift reaction experiment presented in Fig. 13a, the system was flushed with He for 1 h at 400 °C. The spectrum taken after 60 min of flushing shows no IR features (Fig. 13b). Subsequently, CO was introduced into the system while the system temperature was maintained at 400 °C. The relative intensities of the CO_2 and CO bands in the spectrum taken in the first 5 min (Fig. 13b) are very similar to those seen after 60 min of steady-state reaction (Fig. 13a). As CO flow continues, the intensity of the CO_2 bands decreases while the intensity of the CO bands increases. After 30 min of CO flow, the system was flushed with He and H_2O was introduced. After 60 min of H_2O flow, the system was flushed again with He for 60 min. The spectrum taken at this point shows no spectral features. Subsequently CO was introduced into the system again. It can be seen that the relative intensities of CO_2 and CO are essentially the same as in the previous run with CO. The DRIFT results show that the catalyst surface is capable of providing oxygen to the CO molecule even when there is no water in the system. This reaction depletes the oxygen available in the catalyst. When the surface comes in contact with H_2O, the oxygen is replenished returning the surface to the same state as before.

There are two possible reaction mechanisms of the HTS reaction that have been proposed over Fe-based catalysts, associative and regenerative (redox) [32]. The associative mechanism involves the adsorption of CO and H_2O on the catalyst surface, leading to the formation of an intermediate (i.e., formate), which subsequently decomposes to CO_2 and H_2. The redox mechanism can be visualized as a cyclic change in the oxidation state of iron in the magnetite phase upon adsorption of H_2O and CO, consecutively. The redox mechanism seems to be the predominant reaction pathway due to the unique capability of magnetite to exchange an electron between Fe^{2+} and Fe^{3+} sites rapidly. Magnetite is known to have an inverse spinel structure [33,34]. It consists of Fe^{3+} located in tetrahedral sites with octahedral sites

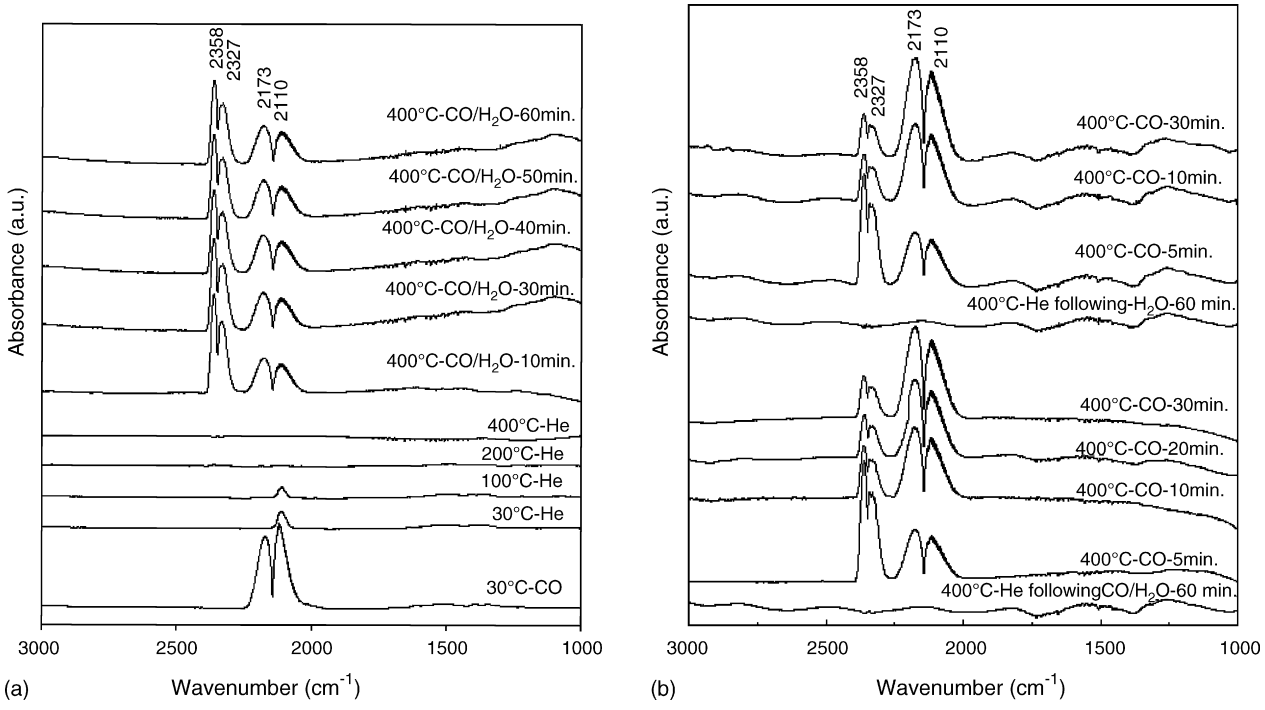

Fig. 13. DRIFT spectra of species from CO adsorption and water gas shift reaction over reduced Fe–Al–Cu (one-step) catalyst. (a) CO flow at 30 °C followed by He flushing and heating to 400 °C and WGS at 400 °C. (b) He flushing the above system followed by CO flow, H_2O flow, and CO flow cycle.

occupied by Fe^{2+} and Fe^{3+} equally, while the oxygen atoms form a face-centered cubic lattice (fcc) within the spinel. The arrangement of iron and oxygen atoms in magnetite can be written as $Fe_{(A)}{}^{3+}Fe_{(B)}{}^{3+}Fe_{(B)}{}^{2+}(O^{2-})_4$, where A and B refer to tetrahedral and octahedral sites, respectively. Fast electron hopping between Fe^{2+} and Fe^{3+} located in octahedral sites in magnetite has been confirmed by Mössbauer spectroscopy [35,36] and isotopic labeling studies [37]. Furthermore, the water-gas shift reaction over Fe–Cr catalysts was well described by the kinetics of surface oxygen removal by CO and surface oxygen incorporation from H_2O, indicating that the redox mechanism is the primary pathway for the water-gas shift reaction over magnetite [38,39]. Our reaction results and XPS characterization indicate that magnetite is the major catalytic phase. *In situ* DRIFTS results show that the WGS reaction over Fe-based catalysts occurs via the redox mechanism. The catalyst surface undergoes successive oxidation and reduction cycles by H_2O and CO to produce H_2 and CO_2 respectively, with Fe^{2+} and Fe^{3+} occupying the octahedral sites in the magnetite structure constituting an oxidation-reduction pair (redox).

The role of copper in HTS catalysts for the water-gas shift reaction is still uncertain. Hutchings and co-workers [15,16] reported that copper enhanced the WGS activity by modifying the electronic properties of coprecipitated Fe–Cr catalysts. Their TPR studies using 5% H_2/Ar and 5% CO/He showed that no additional feature was observed with coprecipitated Fe–Cr–Cu catalyst, suggesting that CuO and Cr_2O_3 could exist within the magnetite structure. TPR profile reported by Araujo and Rangel [18] showed a major reduction peak from reduction of Cu species over Fe–Al–Cu catalyst, which was prepared by coprecipitation of Fe and Al and impregnation of Cu to Fe–Al. They concluded that copper itself does not have a significant role as an active site, but rather as a promoter. Andreev et al. [3] suggested that Cu doped on coprecipitated Fe–Cr catalyst is providing new active sites and reacting in a similar manner as the Cu species in the low temperature Cu/ZnO water gas shift catalyst.

In this study, Fe–Al–Cu (two-step) catalyst was prepared by a coprecipitation–impregnation method by which the catalyst surface could be enriched in copper upon the impregnation step. As previously discussed, TPR, *in situ* XRD, and XPS results clearly indicate that copper is in a metallic form after reduction. This catalyst showed very high activity at lower temperature. The sintering of metallic Cu could contribute to loss of the WGS activity when these catalysts are used at higher temperatures. Therefore, the promotional effect of Cu in these catalysts could be to provide additional active sites for the water-gas shift reaction. For the Fe–Al–Cu (one-step) catalyst prepared by a coprecipitation method, however, XPS and TPR studies indicate that the environment of Cu species in the one-step catalyst is significantly different from that in the two-step catalyst, although, the major Cu species after reduction is also metallic Cu. It is conceivable that with one-step preparation, Cu species co-precipitate with iron oxide to form a solid solution. These Cu species can be reduced to metallic Cu, which provides additional active sites, giving a significant boost to the activity of the catalyst, especially at lower temperatures. At higher temperatures, the sintering of this metallic Cu species is not very extensive as the surface metallic Cu that forms in the two-step preparation because of the spacer function of iron oxide. This could explain why the catalyst prepared by one-step technique has high activity in the entire reaction temperature range investigated in this study. The minor Cu species that cannot be reduced may also contribute to the high activity by providing electronic promotion on magnetite structure. The next paper in this series will report the synthesis of catalysts with well-dispersed Cu species in iron oxide matrix and the electronic function of Cu promoter on the magnetite structure.

4. Summary

Chromium-free iron-based HTS catalysts were prepared by adding both aluminum and copper using two-step coprecipitation–impregnation and one-step coprecipitation methods. The addition of aluminum stabilizes the magnetite phase by retarding its further reduction to FeO or metallic iron. Aluminum is a promising chromium replacement to act as a textural promoter for iron-based water gas shift catalyst. Copper can be used as a structural promoter for high temperature Fe-based catalyst to enhance the catalytic activity. However, the promotion of Cu species is affected by preparation methods significantly. With two-step preparation, the major portion of Cu species is on the iron oxide surface, which is reduced to metallic Cu after reduction. The main promotion of the Cu species in this preparation is to provide additional active sites. With increasing reaction temperature, the promotional effect of Cu decays because of sintering of the metallic Cu, the same phenomenon observed in low temperature water gas shift catalysts. With one-step preparation, the major portion of Cu species coprecipitates with iron oxide. This Cu species is also reduced to metallic Cu at reaction conditions to provide additional active sites. However, this Cu species is not as prone to sintering as the surface Cu due to the spacer function of the iron oxide. A portion of Cu species that cannot be reduced may be incorporated into iron oxide matrix and may serve as an electronic promoter. The *in situ* DRIFTS and XPS studies support the conclusion that the WGS reaction on iron-based catalysts occurs through a redox process on magnetite phase.

Acknowledgments

The financial contributions from the Ohio Coal Development Office and the Ohio Department of Development through the Wright Center of Innovation Program are gratefully appreciated.

References

[1] N.A. Koryabkina, A.A. Phatak, W.F. Ruettinger, R.J. Farrauto, F.H. Ribeiro, J. Catal. 217 (2003) 233.
[2] G.C. Chinchen, R.H. Logan, M.S. Spenser, Appl. Catal. 12 (1984) 89.
[3] A. Andreev, V. Idakiev, D. Mihajlova, D. Shopov, Appl. Catal. 22 (1986) 385.
[4] J.C. Gonzalez, M.G. Gonzalez, M.A. Laborde, N. Moreno, Appl. Catal. 20 (1986) 3.
[5] G. Doppler, A.X. Trautwein, H.M. Ziethen, E. Ambach, R. Lehnert, M.J. Sprague, U. Gonser, Appl. Catal. 40 (1988) 119.

[6] R.L. Keiski, T. Salmi, Appl. Catal. A 87 (1992) 185.
[7] M.C. Rangel, R.M. Sassaki, F. Galembeck, Catal. Lett. 33 (1995) 237.
[8] Y. Li, L. Chang, Ind. Eng. Chem. Res. 35 (1996) 4050.
[9] R.L. Keiski, T. Salmi, P. Niemisto, J. Ainassaari, V.J. Pohjola, Appl. Catal. A 137 (1996) 349.
[10] L.S. Chen, G.L. Lu, J. Mater. Sci. 34 (1999) 4193.
[11] E.B. Quado, M.L.R. Dias, A.M.M. Amorim, M.C. Rangel, J. Braz. Chem. Soc. 10 (1999) 51.
[12] Y. Hu, H. Jin, J. Liu, D. Hao, Chem. Eng. J. 78 (2000) 147.
[13] P. Kappen, J.D. Grunwaldt, B.S. Hammershoi, L. Troger, B.S. Clausen, J. Catal. 198 (2001) 56.
[14] C. Rhodes, B.P. Willaims, F. King, G. Hutchings, Catal. Commun. 3 (2002) 381.
[15] M.A. Edwards, D.M. Whittle, C. Rhodes, A.M. Ward, D. Rohan, M.D. Shannon, G.J. Hutchings, C.J. Kiely, Phys. Chem. Chem. Phys. 4 (2002) 3902.
[16] C. Rhodes, G.J. Hutchings, Phys. Chem. Chem. Phys. 5 (2003) 2719.
[17] D.G. Rethwisch, J. Phillips, Y. Chen, T.F. Hayden, J.A. Dumesic, J. Catal. 91 (1985) 167.
[18] G.C. Araujo, M.C. Rangel, Catal. Today 62 (2000) 201.
[19] J.L.R. Costa, G.S. Marchetti, M.C. Rangel, Catal. Today 77 (2002) 205.
[20] U.S. Ozkan, Y. Cai, M.W. Kumthekar, L. Zhang, J. Catal. 142 (1993) 182.
[21] D.E. Ridler, M.V. Twigg, in: M.V. Twigg (Ed.), Catalyst Handbook, Wolfe, London, 1989, p. 225.
[22] D.S. Newsome, Catal. Rev. Sci. Eng. 21 (1980) 275.
[23] Agency for Toxic Substances and Disease Registry, Toxicological Profile for Chromium, TP-92/08, ATSDR, Atlanta, GA, 1993, p. 227.
[24] J.E. Huheey, E.A. Keiter, R.L. Keiter, Inorganic Chemistry: Principle of Structure and Reactivity, 4th ed., Harper Collins, New York, NY, 1993.
[25] K. Kochloefl, in: G. Ertl, H. Knozinger, J. Weitkamp (Eds.), Handbook of Heterogeneous Catalysis, vol. 4, VCH, Germany, 1997, p. 1819.
[26] B.D. Cullity, Elements of X-Ray Diffraction, 2nd ed., Addison-Wesley, Massachusetts, 1978.
[27] P.H. Emmett, J. Am. Chem. Soc. 55 (1933) 1376.
[28] E.D. Eastman, J. Am. Chem. Soc. 44 (1922) 975.
[29] A. Erdohelyi, K. Fodor, S. Suru, Appl. Catal. A 139 (1996) 131.
[30] H. Kusama, K.K. Bando, K. Okabe, H. Arakawa, Appl. Catal. A 197 (2000) 255.
[31] D. Bianchi, T. Chafik, M. Khalfallah, S. Jean, Appl. Catal. A 105 (1993) 223.
[32] C. Rhodes, G. Hutchings, A.M. Ward, Catal. Today 23 (1995) 43.
[33] R.W. Grimes, A.B. Anderson, A.H. Heuer, J. Am. Chem. Soc. 111 (1989) 1.
[34] G.R. Lumpkin, Prog. Nucl. Energy 38 (2001) 447.
[35] H. Topsoe, J.A. Dumesic, M. Boudart, J. Catal. 28 (1973) 477.
[36] D.G. Rethwisch, J.A. Dumesic, Appl. Catal. 21 (1986) 97.
[37] M. Tinkle, J.A. Dumesic, J. Catal. 103 (1987) 65.
[38] J.E. Kubsh, J.A. Dumesic, AIChE J. 28 (1982) 793.
[39] C.R. Lund, J.E. Kubsh, J.A. Dumesic, in: R.K. Grasselli, J.F. Brazdil (Eds.), Solid State Chemistry in Catalysis, vol. 279, American Chemical Society, Washington, DC, 1985, p. 19.